Cyclic Peptides for Effective Treatment in a Long-Term Model of Graves Disease and Orbitopathy in Female Mice

Hans-Peter Holthoff,[1] Zhongmin Li,[1] Julia Faßbender,[1] Andreas Reimann,[1] Kristin Adler,[1] Götz Münch,[1] and Martin Ungerer[1]

[1]Procorde-advanceCOR, D 82152 Martinsried, Germany

A model for human Graves disease in mice was used to compare several treatment approaches. The mice received regular adenovirus (Ad) thyroid-stimulating hormone receptor (TSHR) A subunit immunizations (injections every 4 weeks). The generation of anti-TSHR antibodies, enlarged thyroid sizes (goiter), elevated serum thyroxine levels, retro-orbital fibrosis, and cardiac involvement (tachycardia and hypertrophy) were consistently observed over 9 months. Treatment of established disease in these mice using cyclic peptides that mimic one of the cylindrical loops of the TSHR leucine-rich repeat domain improved or cured all investigated parameters after six consecutive monthly injections. Substantial beneficial effects were observed 3 to 4 months after starting these therapies. In immunologically naive mice, administration of any of the cyclic peptides did not induce any immune response. In contrast, monthly injections of the full antigenic TSHR A domain as fusion protein with immunoglobulin G (IgG)-Fc induced clinical signs of allergy in Ad-TSHR–immunized mice and anti-TSHR antibodies in naive control mice. In conclusion, cyclic peptides resolved many clinical findings in a mouse model of established Graves disease and orbitopathy. In contrast to blocking TSHR by allosteric modulation, the approach does not incur a direct receptor antagonism, which might offer a favorable side effect profile. (***Endocrinology*** **158: 1–16, 2017)**

Graves disease is a common antibody-mediated autoimmune condition targeting the thyrotropin–thyroid-stimulating hormone (TSH) receptor (TSHR) in the thyroid gland, resulting in hyperthyroidism (1), with an annual incidence of 15 to 80/100,000 persons worldwide. The disease is often initially treated with thyreostatic drugs, such as carbimazole, followed by radioiodine therapy (2) or surgical removal of the thyroid gland. These treatment options are characterized by relatively high relapse rates and important side effect profiles (3). A quality of life assessment showed that all options are accompanied by reduced vital and mental quality of life even many years after treatment (4). If left untreated, Graves disease leads to significantly increased morbidity and mortality (4).

The treatment of refractory disease cases and accompanying ophthalmopathy and orbitopathy are especially challenging. Ophthalmopathy occurs in almost one half of all patients with Graves disease—≤16/100,000 women annually in the general population (5). In ophthalmopathy, anti-TSHR antibody titers and relapse rates will be especially high (5). These patients must be treated frequently with high doses of intravenous corticoids for many weeks, resulting in more side effects (6). Therefore, novel treatment options have been explored in recent years. A reduction in B lymphocytic cell counts can be achieved with the anti-CD20 antibody rituximab (MabThera; anti-CD20 monoclonal antibody). Driven by the hypothesis that Graves disease is mostly a B-cell–mediated condition, several smaller observational studies (7, 8) investigated administration of rituximab to patients with refractory Graves ophthalmopathy. Two recent randomized double-blind trials yielded disparate results: one

ISSN Print 0013-7227 ISSN Online 1945-7170
Printed in USA

Received 15 November 2016. Accepted 23 March 2017.
First Published Online ■■■ ■■■ 2017

Abbreviations: Ad, adenovirus; ANOVA, analysis of variance; β1AR, β1 adrenergic receptor; cAMP, cyclic adenosine monophosphate; CHO, Chinese hamster ovary; DMF, *N*,*N*-dimethylformamide; ECG, electrocardiogram; ELISA, enzyme-linked immunosorbent assay; FMOC, fluorenylmethoxycarbonyl; IgG, immunoglobulin G; LRD, leucine-rich domain; PBS, phosphate-buffered saline; T4, thyroxine; TSH, thyroid-stimulating hormone; TSHR, thyroid-stimulating hormone receptor.

showed an advantage for the rituximab-treated group (9); however, the other [6] did not (ClinicalTrials.gov identifier, NCT00595335), perhaps because of the frequent side effects from the therapy.

Because these approaches did not yield clear clinical efficacy and many potential patients declined to participate in the trial for fear of side effects (6), an alternative was offered by specific immune therapies that have been established for allergic autoimmune conditions for >100 years (reviewed by Larché and Wraith [10] and Soyka *et al.* [11]). Increasingly, recombinant peptides have been used for this hyposensitization therapy, which offers substantial advantages compared with the classic raw allergen extracts (10, 12, 13). In general, treatment with broad-range immunosuppressive drugs can cause serious side effects; thus, such allergen-specific therapies are conceived to induce tolerance in a variety of related conditions. As a novel option, Jahns *et al.* (14), Freedman *et al.* (15), Boivin *et al.* (16), Münch *et al.* (17), and Störk *et al.* (18) have established intravenous administration of fairly high doses of immunogen-mimicking cyclic peptides for the treatment of anti-G protein-coupled receptor-mediated autoimmune disease. In the present study, we sought to establish a similar approach for anti-TSHR–mediated disease.

A disease model for human Graves disease was successfully established using up to three immunizations with recombinant adenovirus (Ad) expressing the full-length human TSHR (19) and reconfirmed in further studies using the extracellular A subunit of the TSHR (20). Subsequent studies showed variations in protocol and successful extension with repeated immunization (21, 22). This extended protocol of Ad-induced TSHR immunization (22), in which regular injections are continued for 9 months, was used to permanently boost antibody production in mice. The model established a stable disease phenotype during the whole observation period, including thyroid enlargement (goiter), hyperthyreotic thyroxine (T4) values, tachycardia, and retro-
Q:6 orbital fibrosis. The latter readout indicates the severity of ophthalmopathy, as investigated on histological serial orbital sections (23). This protocol was conceived in parallel with the previously cited studies, which successfully established a long-term disease model of cardiomyopathy caused by anti-β1 receptor antibodies in rats and its treatment with cyclic peptides (14–18).

Using a method similar to that used in the previous study, cyclic peptides that mimic the tertiary structure of the single cylindrical loops of the TSHR leucine-rich repeat domain were designed. These peptides were systematically tested for their potency treat and improve the clinical disease manifestations in TSHR-immunized diseased mice.

In the present study, we show that cyclic peptides that mimic one of the cylindrical loops of the leucine-rich repeat domain of TSHR suppressed, or at least stabilized, the titers of TSH-binding antibodies despite continuing immunizations. Thus, established thyroid disease was successfully treated in these mice, and thyroid hyperplasia and histological alterations were markedly reduced. Elevated T4 levels had normalized, starting 15 weeks after initiation of peptide therapy. We also found that retro-orbital fibrosis was minimized, suggesting a positive effect on Graves orbitopathy. Tachycardia and cardiac hypertrophy were consistently reduced by the peptide therapy. These data include and expand on some preliminary results of a pilot study previously reported in a recent review (23).

Materials and Methods

Recombinant Ad

The DNA sequence coding for the first 289 amino acids of the human TSHR (23, 24) was cloned into the Microbix Admax (Microbix Biosystems, Inc., Mississauga, Ontario, Canada) Ad expression system, as previously reported (22). HEK293A cells were used to propagate until the first viral plaques became visible. This system results in recombinant replication-deficient E1 and E3-deficient Ad type 5. A control Ad containing only the reporter gene GFP (Ad-GFP) was amplified and purified in the Q:7 same manner.

Synthesis of cyclic peptides

Cyclic peptides with structural homology to the 10 cylindrical loops of the TSHR leucine-rich domain were designed as outlined in Table 1. Specifically, the sequence of peptide 836 replicates the eighth cylindrical loop, and peptide 829 was

Table 1. TSHR Peptides, Head-to-Tail Cyclization

Peptide No.	Derived From TSHR Sequence aa	Meric Peptide
829	26-49	SPPCECHQEEDFRVTCKDIQRIPS Q:23
830	50-73	LPPSTQTLKLI ETHLRTIPSHAFS
831	73-89	SNLPNISRIYVSIDVTL
832	98-121	YNLSKVTHIEIRNTRNLTYIDPDA
833	122-145	LKELPLLKFLGIFNTGLKMFPDLT
834	146-163	KVYSTDIFFILEITDNP
835	170-193	NAFQGLCNETLTLKLYNNGFTSVQ
836	194-217	GYAFNGTKLDAVYLNKNKYLTVID
837	218-237	KDAFGGVYSGPSLLDVSQTS
838	242-265	PSKGLEHLKELIARNTWTLKKLPL

TSHR amino acid (aa) sequences from which cyclic peptides used in the study were derived. After synthesis, each peptide was cyclized head-to-tail. Each peptide approximates 1 of the 10 loops of the leucine-rich region of TSHR domain A. In accordance with the amino acid length of these loops, 24-meric peptides were used, with the exception of peptides derived from the third, sixth, and ninth loop. For technical reasons, cyclic 24-meric could not be provided for these loops; thus, the 17-meric (third and sixth loop) or 20-meric (ninth loop) peptides were used instead.

designed in analogy to the first loop of the TSHR leucine-rich repeat domain. In view of its biological inactivity, peptide 835 was used as an additional inactive control cyclic peptide in the present study. They were synthesized by BIOSYNTAN (Berlin, Germany) according to the described protocols for fluorenylmethoxycarbonyl (FMOC) resin-based amino acid chain elongation and subsequent head-to-tail cyclization. FMOC amino acid or FMOC dipeptide was attached to the 2-chlorotrityl chloride resin (RAPP Polymere GmbH, Tuebingen, Germany) yielding a loading of 0.30 mmol/g resin. Peptide synthesis was performed by a standard cycle of deblocking with 30% piperidine/*N,N*-dimethylformamide (DMF; 5+12 minutes) and coupling with 3 equivalents (eq) FMOC amino acid/*O*-(7-azabenzotriazol-1-yl)-*N,N,N′,N′*-tetramethyluronium-hexafluorphosphate/6 eq *N*-methylmorpholine in DMF (double coupling, 2 × 30 minutes). After cleavage from the resin by 20% hexafluoroisopropanol/DCM (2 × 20 minutes), the isolated crude peptide was cyclized by 1.5 eq 7-azabenzotriazol-1-yloxy) tripyrrolidinophosphonium hexafluorophosphate/3 eq *N,N*-diisopropylethylamine in DMF overnight, the solvent was evaporated, and the crude peptide was deblocked by trifluoroacetic acid/water/thioanisole (95:5:3 v/v/v) for 2 hours. Next, the peptides were purified to ≤95% using high-performance liquid chromatography and analyzed using matrix-assisted laser desorption/ionization time of flight mass spectrometry. This quality control reconfirmed that the amino acids had been correctly included into the peptides, and their cyclization was evident from the experimental determination vs theoretical prediction of the molecular weight. For example, the value of observed vs predicted molecular weight was 2703.2 vs 2703.2 for peptide 836, 2800.0 vs 2800.0 for peptide 829, and 2657.0 vs 2657.1 for control peptide 835.

Expression and purification of TSHR fusion protein

The fusion protein consisted of the first 289 amino acids of the human TSHR (extracellular TSHR A subunit) followed by a GGR linker and the Fc portion of human IgG2. The complementary DNA sequence adapted for hamster codon usage was produced synthetically and cloned into the plasmid vector pcDNA5/FRT. This expression vector was transfected into Chinese hamster ovary (CHO) Flp-In cells, together with the plasmid pOG44, providing site-directed recombination. After selection of a stably expressing clone, the fusion protein was purified from suspension culture supernatant using ProteinG chromatography and dialyzed against phosphate-buffered saline (PBS).

Studies in immunized mice

Female BALB/c mice were delivered from Charles River Laboratory (Sulzfeld, Germany) and allowed to adapt for ≥1 week before the start of the experiments at the age of 6 weeks. The mice were kept under standard housing conditions (23° ± 2°C, 55% ± 10% relative humidity) in groups of 10 animals in GR1800DD cages (Tecniplast®, West Chester, PA). The local animal welfare authority and ethics committee at the Regierung von Oberbayern (Government of Upper Bavaria, Munich, Germany) approved all animal experiments (approval no. 55.2-1-54-2531-25-12), which were performed in accordance with the Declaration of Helsinki of the World Medical Association, and the European Commission guidelines (Directive 2010/63/EU). All guidelines for the care of animals were respected.

The mice received 10^{10} plaque-forming units of Ad carrying the A-subunit of the TSHR gene. In addition, age-matched immunologically naïve mice were studied for comparison. For immunization, the mice were anesthetized with isoflurane (introduction 5%, maintenance 1.5% to 2%) and placed on a heating pad. The Ad was injected into the left and right femoral muscles at a volume of 25 μL each.

For blood withdrawal, the mice were moved to a restrainer, and 100 μL of blood was withdrawn from the left or right tail vein with a 27-gauge needle. The blood samples were centrifuged at 2400*g* for 15 minutes at room temperature, and the serum was stored at −20°C. At the end of the study (before euthanasia), blood was withdrawn intracardiacally with the mouse under deep anesthesia (170 mg/kg ketamine plus 17 mg/kg xylazine) using a 1-mL syringe and a 24-gauge needle. These samples were also centrifuged at 2400*g* for 15 minutes at room temperature and the serum stored at −20°C.

The study protocol used three immunizations every 3 weeks ("initiation"), followed by a "maintenance" phase with additional regular boosts every 4 weeks until the ninth immunization, as described previously (22). The mice were randomly assigned to therapeutic groups. Therapy (either 1 mg/kg body weight peptides or 0.9% NaCl vehicle control) was given 1 week after the fourth immunization by intravenous injection into a tail vein and continued at 4-week intervals, as described previously for treatment of anti–β1 adrenergic receptor (β1AR) (16). The fusion protein TSHR-Fc was given intravenously at identical times at a dose of 1 mg/kg. The fusion protein was administered with the histamine receptor blocker clemastine (Tavegil) at a dose of 0.02 mg per mouse (25 g body weight) to avoid the clinical symptoms of an allergic reaction, which had been observed in initial pilot studies of TSHR-Fc administration in mice. A detailed immunization schedule is shown in Fig. 1(a).

The heart function of the mice undergoing anesthesia for immunization was monitored using electrocardiography (ECG amplifier module; Harvard Apparatus; Hugo Sachs Electronik, March, Germany) and recorded using a special software program, which allows one to determine the heart rate from the ECG reading (Haemodyn; Hugo Sachs Electronik). ECG was also performed during anesthesia before the mice were euthanized for histological examination at the end of the study.

Studies in native mice

BALB/c mice were allowed to adapt for ≥1 week before the start of the experiments at the age of 12 weeks. The mice were maintained as described previously. The local animal welfare authority and ethics committee at the Regierung von Oberbayern (Government of Upper Bavaria, Munich, Germany) also approved these experiments (approval no. 55.2-1-54-2532.0-32-15), which were performed in accordance with the European Commission guidelines.

Peptides (either 1 mg/kg body weight or NaCl vehicle control) were given by intravenous injection into a tail vein of these naïve mice (n = 6 per group) and continued at 4-week intervals for 6 months, as described for the therapeutic study of immunized mice. Serum samples were taken at identical intervals.

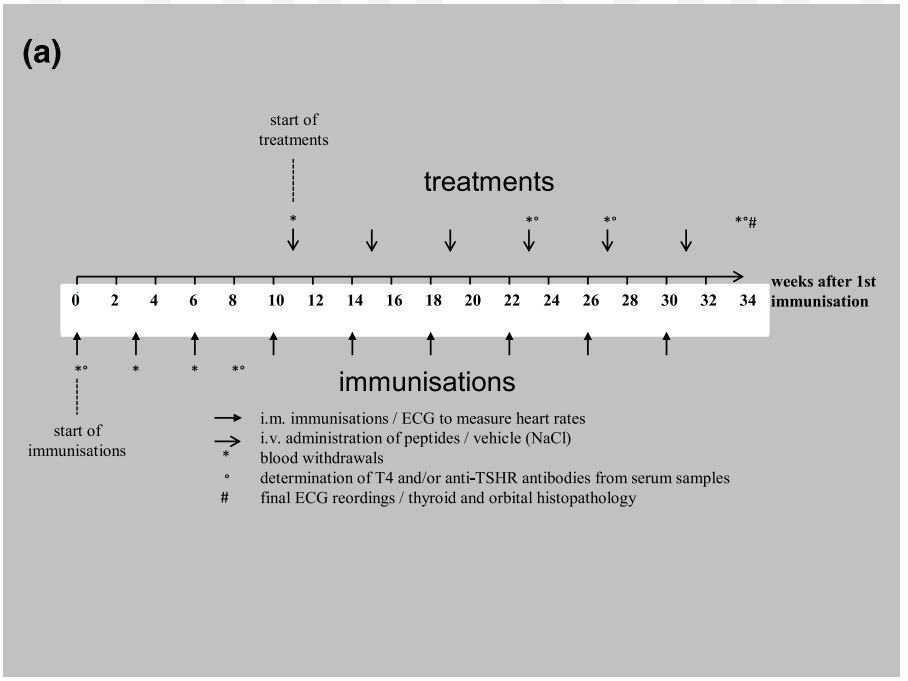

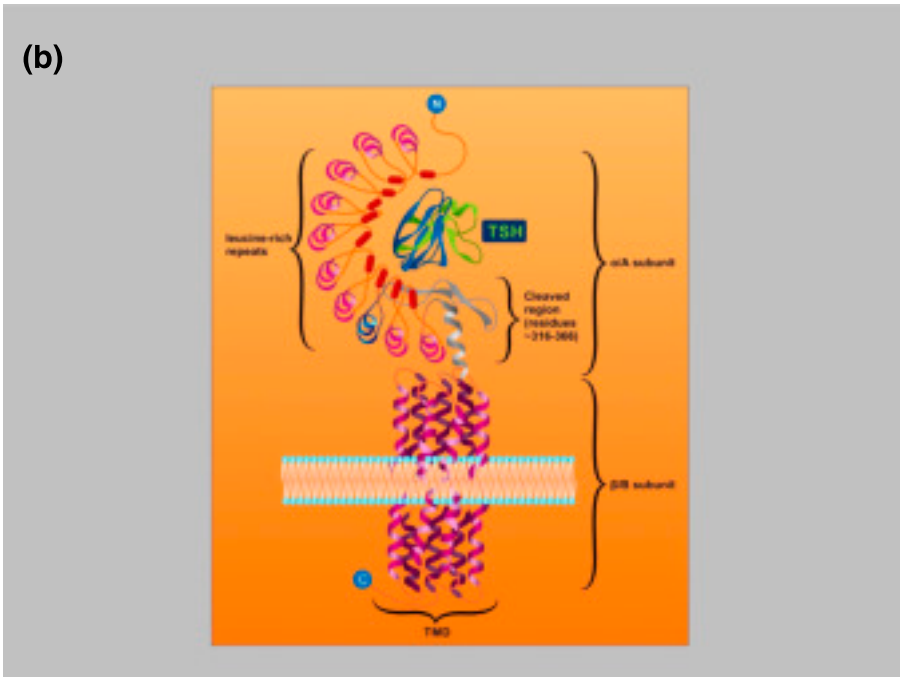

Figure 1. (a) Time schedule of the study for immunization, administration of therapeutic peptides, and measurements. (b) Schematic structure of TSHR. Cyclic peptides were derived from the loop structure of the leucine-rich repeat domain of the extracellular A subunit of the TSHR (marked in blue). i.m., intramuscular; i.v., intravenous; TMD, transmembrane domain.

Measurements in mouse sera

Anti-TSHR autoantibody titers and the potency of antibodies to stimulate TSHR-dependent cyclic adenosine monophosphate (cAMP) levels in test cells were determined before the start of immunization (basal value), 56, 133, and 189 days after the first immunization, and at the end of the experiment. Two different assays were used:

1. Third-generation assay: antibodies against TSHR were detected using a commercially available third-generation enzyme immunoassay (RSR Limited, Cardiff, UK), in which the human Graves patient-derived M22 monoclonal antibody and serum antibodies compete for binding sites on immobilized TSHR. The assay is also used in the Roche Cobas assay (model no. 04388790; Roche Diagnostics, Indianapolis, IN) for electrochemiluminescence immunoassay, with minor modifications. The assay was performed using 30 μL 1:10 v/v (PBS) diluted serum in at least double

determination, according to the manufacturer's instructions.

2. Thyroid-stimulating antibodies in the serum of hyperthyroid mice were analyzed by measuring cAMP generation in CHO JP2626 cells expressing the human TSHR (provided by Dr. Gilbert Vassart, Brussels, Belgium). The CHO cells were seeded onto 96-well plates (30,000 cells per well) and incubated for 24 hours in Dulbecco's modified Eagle medium (Invitrogen, Carlsbad, CA) containing 2% fetal calf serum. Next, Dulbecco's modified Eagle medium was removed and mice serum was diluted 1:8 in 40 μL Hanks balanced salt solution buffer (20 mM Hepes, 1.26 mM $CaCl_2$, 5.33 mM KCl, 0.44 mM KH_2PO_4, 0.5 mM $MgCl_2$, 0.4 mM $MgSO_4$, 4.2 mM $NaHCO_3$, 5.6 mM glucose, and 222 mM sucrose; pH 7.2) supplemented with 1.5% bovine serum albumin and 0.5 mM isobutyl-1-methylxanthine (Sigma-Aldrich, Pole, UK) and added to each well. After incubation for 2.5 hours at 37°C, the cAMP release in the medium was measured in duplicate using a competitive immunoassay, enzyme-linked immunosorbent assay (ELISA; model no. EMSCAMPL; Thermo Fisher Scientific Life Sciences, Waltham, MA).

Total T4 was measured using an immunoassay kit (model no. T4044T-100; Calbiotech Inc., Austin, CA) in duplicate determination.

Histological analysis

After euthanasia, dissection of the thyroid glands was performed under a stereomicroscope, as described previously (22). In brief, cross cuts at the level above the larynx and below the seventh cartilage ring were made, and the gland with the tracheae and esophagus was removed from the neck. Tissue blocks were kept in 4% neutral paraformaldehyde, washed in PBS three times, and embedded in optimum cutting temperature formulation (Tissue-Tek O.C.T. compound; VWR Chemicals, Leuven, Belgium). Consecutive 5-μm-thick cross sections were cut at a fixed distance of 500 μm using a Leica microtome CM1850 cryostat (temperature, −19°C; Leica Biosystems, Buffalo Grove, IL) and mounted on Polysine slides (catalog no. J2800AMNZ; Thermo Fisher Scientific Life Sciences). The collected sections represented a total distance of ~5 to 6 mm and covered the whole thyroid region of each animal. The tissue sections were stained with hematoxylin and eosin and examined using bright field illumination on a Zeiss upright microscope (Carl Zeiss AG, Oberkochen, Germany). The thyroid volumes (mm^3) were calculated from the sum of the areas of each section over the whole cutting region.

The myocardial volumes (mm^3) were calculated from the sum of the areas of each section over whole cutting region (five to six slides, depending on size of the heart), similar to the method described for the thyroid glands, as described previously (22).

For orbital preparations, complete dissection of the orbital and periorbital areas was performed, collecting all orbital tissues, eyelids, and adjacent tissues. Consecutively, the tissues were trimmed, fixed, and decalcified by placing in EDTA solution (15%; pH 7.0) for 48 hours and then washed three times with PBS. Next, the tissues were immerged in a sucrose solution (30% in PBS) for 24 hours at 4°C, followed by fine trimming and incubating in optimum cutting temperature formulation (Tissue-Tek O.C.T. compound; VWR Chemicals) for 5 minutes at room temperature. Special care was taken to embed the optical nerve side upside down. Using the microtome, we performed serial coronary sections (7 μm thick, 0.63 mm apart). Cutting was started at the level of bregma 0 and sections were collected at positions (compared with bregma 0) +0.63, +1.26, +1.89, +2.52, +3.15, +3.78, +4.41, and +5.04 mm (shown in later figure). The sections were stored at −70°C until use. Then, Q:12,13 they were thawed to room temperature for 30 minutes and stained with hematoxylin and eosin. For Masson's staining, the sections were placed in Bouin fixation solution (containing 30 mL of saturated picric acid, 10 mL of concentrated formaldehyde, 2 mL of glacial acetic acid) at 20°C overnight and washed under running tap water for 2 hours. Next, the sections were treated using the Masson-Goldner trichrome staining kit (catalog no. 3459.1; Roth, Bavaria, Germany) according to the provider's protocol.

The orbital sections were viewed using a 4× objective lens (Axioscope; Carl Zeiss), captured with an Axiovision digital camera system, and recorded with 2560 × 1920 pixel resolution. The focus was adjusted for each new field, but the light conditions were kept identical. All sections were evaluated in a blinded fashion.

The areas of fibrosis in the extraorbital adipose tissue and extraorbital muscle regions are indicated by staining green. Digitized image analysis of the green pixels was performed using the luminescence tool of Adobe Photoshop software, version CS5 (Adobe Systems, San Jose, CA), extended on the basis of pixel areas. To correct for possible bias between staining, the green staining intensity of the respective orbital bone in each section was considered the internal standard for each measurement. Quantification of fibrosis using digitized Adobe Photoshop analysis of Masson's trichrome stain was validated previously (25, 26). Accordingly, all fibrotic tissue throughout a Q:14 whole orbital section was quantified, and the results of all sections were summed to yield a total fibrosis volume (mm^3) for each investigated orbit (considering the 0.63-mm thickness between sections).

In vitro studies

To investigate the direct binding of peptides to anti-TSHR antibodies, the Roche Cobas assay (model no. 04388790) for electrochemiluminescence immunoassay was used, with minor modifications: 30 μL of the diluted monoclonal M22-Bio antibody was mixed with 30 μL diluted peptide or TSHR-Fc (final concentration of 100 μg/mL in PBS) and added to the TSHR-precoated microtiter plate. After an incubation step for 2 hours at room temperature, the protocol was continued according to the manufacturer's instructions.

To investigate effects on TSHR-dependent cAMP stimulation *ex vivo*, TSHR-overexpressing CHO JP2626 cells were prepared as described. Next, 100 μg/mL peptide 829, peptide 836, or fusion protein TSHR-Fc was added to the JP2626 cells. After incubation for 2.5 hours at 37°C, the cAMP release in the medium was measured in duplicate using a competitive immunoassay, ELISA (model no. EMSCAMPL; Thermo Fisher Scientific Life Sciences).

Statistical analysis

Differences between the groups were analyzed using analysis of variance (ANOVA) for comparison between groups using SPSS software, version 19 (IBM Corp., Armonk, NY), followed by least significant difference *post hoc* test or Student *t* test, as appropriate. For comparison of values at various times within one group, ANOVA for repeated measurements was used, as appropriate.

Results

Selection of cyclic peptides

Cyclic peptides whose amino acid sequences and tertiary structures were derived from each of the 10 loops of TSHR leucin-rich domain (LRD) were synthetized (Table 1). Peptide 836 is a 24-meric cyclic peptide corresponding to the eighth TSHR LRD loop, and peptide 829 (also 24-meric) corresponds to the first loop of the TSHR LRD. As an example for an inactive control, peptide 835, whose sequence was derived from the seventh loop, was included in the additional results. All three peptides were easily soluble in water; thus, 0.9% NaCl was used as the vehicle and for TSHR-Fc.

Anti-TSHR antibody titers and capacity to stimulate cAMP in test cells

Anti-TSHR antibodies were determined from serum samples by investigating the ability of the respective mouse sera to inhibit the binding of the monoclonal Graves patient antibody M22 to the TSHR (third-generation ELISA). Highly substantial titers were detected in all Ad-TSHR–immunized animals. In the mock-treated group, the mean anti-TSHR antibody titers increased progressively during the course of the study (Fig. 2). In contrast, peptide 836-treated and TSHR-Fc–treated mice showed no trends for additional anti-TSHR titer increases after the start of therapy despite continuing immunizations. The titers in the peptide 829-treated mice were similar to those in the untreated control group.

In addition, the stimulatory activity of these antibodies was determined as the capacity of mouse serum samples to induce an increase in TSHR-dependent cAMP levels in test cells (Fig. 3). Anti-TSHR antibodies from almost all TSHR-immunized mice showed potency to stimulate cAMP in TSHR-expressing test cells. The maximum inducible cAMP levels showed considerable variation. Cyclic peptide therapy did not affect these mean cAMP values. A trend toward somewhat lower TSHR-cAMP

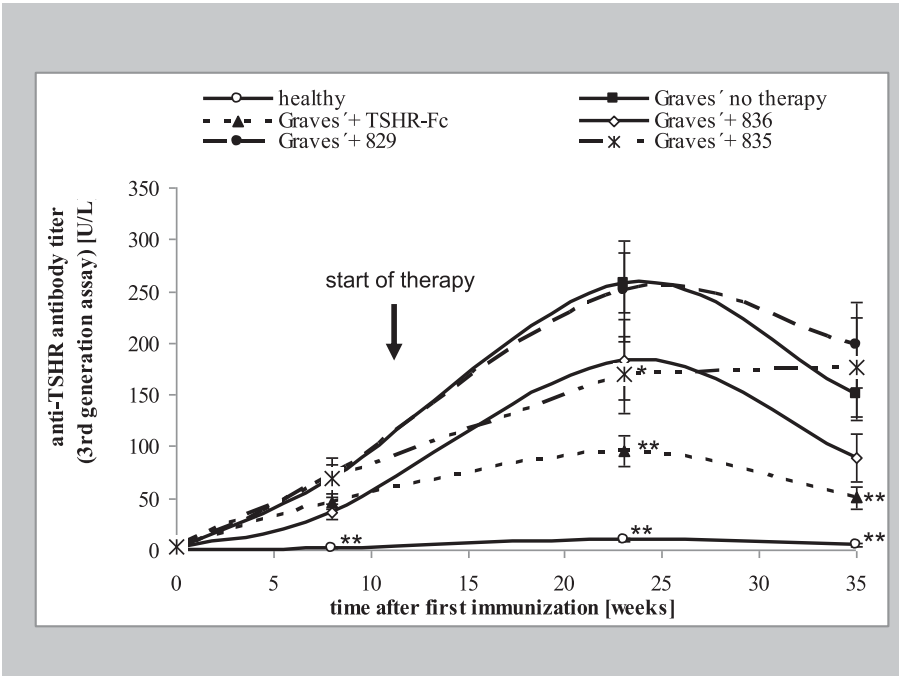

Figure 2. Effect of peptide therapy on anti-TSHR antibody titers measured using third-generation ELISA, in which serum samples are used to determine inhibition of M22-binding to coated plates. The measurements were performed in Ad-TSHR–immunized mice treated by injections of vehicle (0.9% NaCl; "Graves no therapy"; n = 25 mice) or 1 mg/kg body weight of peptide 836 (n = 12 mice), peptide 829 (n = 13 mice), TSHR-Fc (n = 18 mice), or control peptide 835 (n = 13 mice) at 4-week intervals. In addition, age-matched immunologically naive unimmunized mice ("healthy"; n = 19 mice) were investigated. Data presented as mean ± standard error of mean. Significance over time was tested by ANOVA of groups at given time points and controlled by ANOVA for repeated measurements within one group, followed by least significant difference *post hoc* testing. $*P < 0.05$ and $**P < 0.005$, compared with the TSHR-immunized group treated with only NaCl ("Graves no therapy" group).

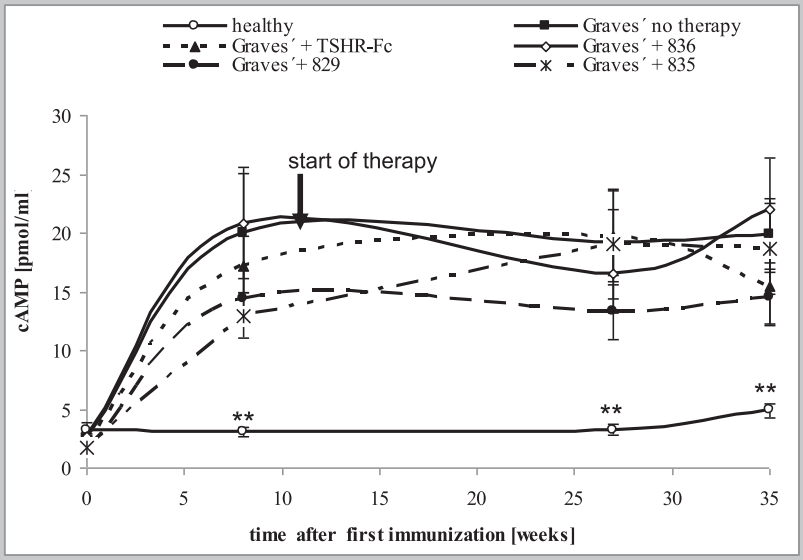

Figure 3. Effect on cAMP stimulation in TSHR-expressing test cells, as determined in sera from mice during the experiment. The effects of peptide therapy on the capacity of anti-TSHR antibodies to stimulate cAMP generation were evaluated in CHO cells expressing human TSHR. The measurements were performed in Ad-TSHR–immunized mice treated by injections of vehicle (0.9% NaCl; "Graves no therapy" group; n = 25 mice) or 1 mg/kg body weight of peptide 836 (n = 12 mice), peptide 829 (n = 13 mice), TSHR-Fc (n = 18 mice), or control peptide 835 (n = 13 mice) at 4-week intervals. In addition, age-matched immunologically naive unimmunized mice ("healthy"; n = 19 mice) were investigated. Data presented as mean ± standard error of mean. Differences between groups were tested by AVOVA followed by *post hoc* least significant difference testing. $^{**}P < 0.005$ compared with TSHR-immunized group treated with only NaCl ("Graves no therapy" group).

stimulation values for peptide 829 can be seen in Fig. 3. However, the values were not significantly different from those of the controls; thus, the effect was a random group effect, because it had occurred before the start of therapy (evident at week 8).

Thyroid sizes determined macroscopically and from histological sections

The thyroid volumes (mm^3) were determined from the sum of the areas of each section over the whole cutting region (5 to 10 slides, depending on size of the thyroid gland) multiplied by the slice thickness of 0.5 mm. This macroscopic investigation showed clearly increased thyroid glands in mice that had received nine immunizations of Ad-TSHR [Fig. 4(b)] compared with the healthy mouse group. In contrast, peptide 836-treated and TSHR-Fc–treated mice showed decreased thyroid size; the peptide 829-treated mice showed a trend that did not reach statistical significance. Also, other tested cyclic peptides derived from the structure of the TSHR A domain did not show any effects. As an example of an inactive control, the results for peptide 835, whose sequence was derived from the seventh loop, are also shown in Fig. 4(b). Figure 4(a) shows representative macrophotographs of the thyroid glands.

Pathohistological changes in the thyroid

A qualitative histological investigation was also performed in some animals. In nine Ad-TSHR–treated mice, prominent infoldings of the hyperplastic follicular epithelium occurred, which led to fractioning of thyroid follicles and corresponding smaller follicle and colloid sizes (22). This degenerate histological image contrasted with the normal aspect of intact follicles and normal colloid size of native animals. The mean histological scores of the TSHR-Fc–treated groups were markedly better than those of the vehicle-treated group (Supplemental Fig. 1).

Determination of T4 serum levels

The T4 levels did not differ between groups at the study start, and the mean T4 levels in the Ad-TSHR–immunized groups were consistently and significantly greater than controls until week 11 (start of therapy; Fig. 5). Compared with the reported normal values in mice (serum T4 levels >8 μg/dL were considered hyperthyroid in BALB/c mice by most investigators), the T4 levels were consistently increased beyond that cutoff value in these groups. After the start of therapy, the peptide 836-treated and TSHR-Fc–treated mice showed progressively decreasing T4 levels, which consecutively

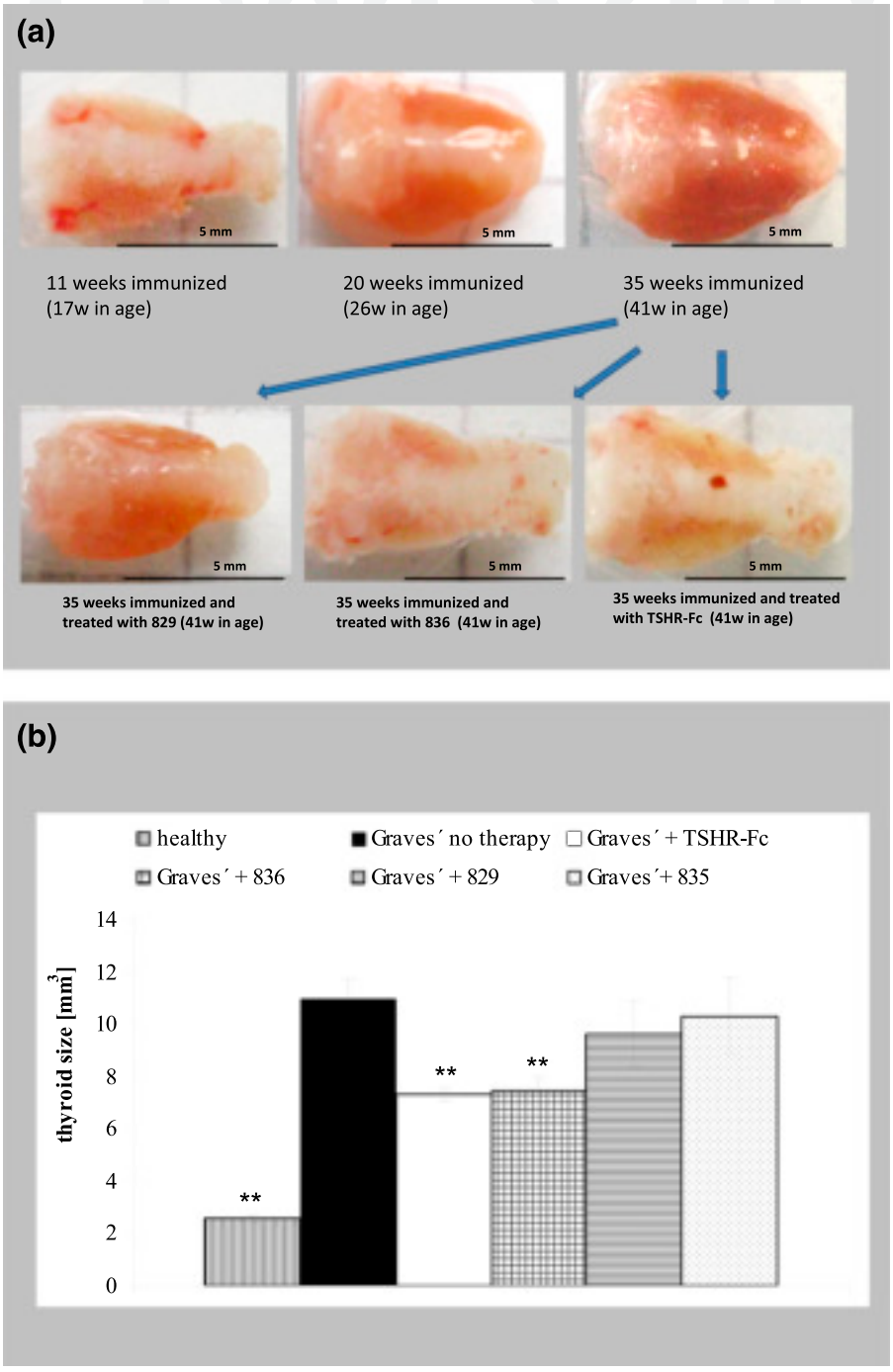

4C

Figure 4. Effect on thyroid size. (a) Representative macroscopic images of effects on thyroid size. Comparison of thyroid glands of mice immunized with Ad-THSR, treated with vehicle NaCl only and killed at various time points (upper) with thyroid gland from a 35-week-old TSHR-immunized mouse treated with TSHR-Fc or peptide 836 or 829 (lower). Representative images shown. (b) Peptide therapy effect on macroscopically measured thyroid size were investigated at the end of the experiment. The measurements were performed in Ad-TSHR–immunized mice treated by injections with vehicle (0.9% NaCl; "Graves no therapy" group; n = 25 mice) or 1 mg/kg body weight of peptide 836 (n = 12 mice), peptide 829 (n = 13 mice), TSHR-Fc (n = 18 mice), or control peptide 835 (n = 13 mice) at 4-week intervals. In addition, age-matched immunologically naive unimmunized mice ("healthy"; n = 9 mice) were investigated. The mean ± standard error of mean thyroid sizes (mm^3). Differences between groups were tested by ANOVA, followed by *post hoc* least significant difference testing. $^{**}P < 0.001$ compared with the TSHR-immunized group treated with only NaCl ("Graves no therapy" group).

reverted to normal values. The mean values were close to those of the healthy animal group at later time points.

In contrast, the peptide 829-treated mice showed a trend that did not reach statistical significance. Also, other tested cyclic peptides derived from the structure of the other loops of the LRD TSHR A did not result in any effects (as an example of an inactive control, the results

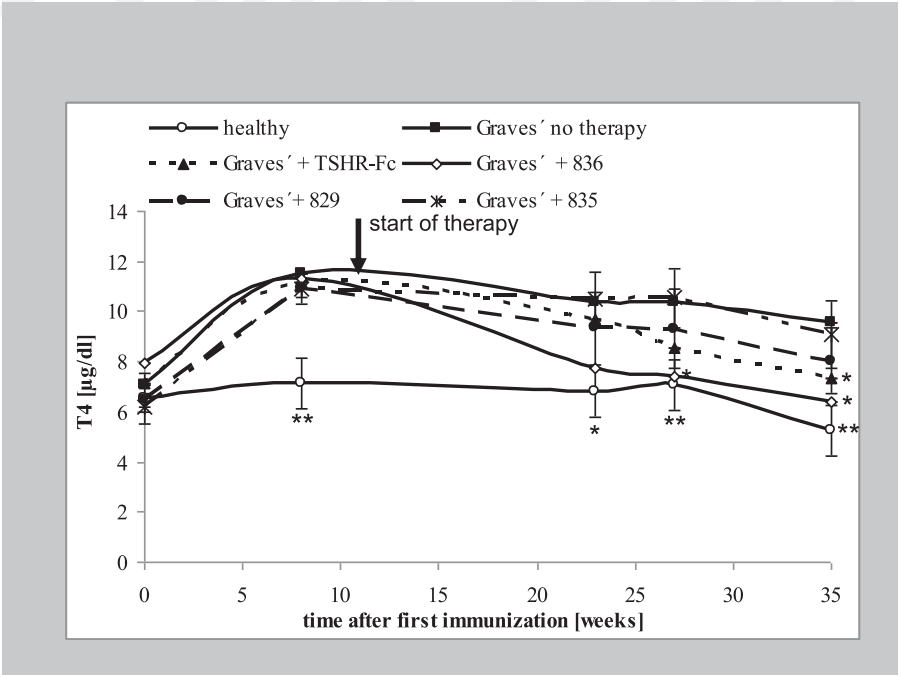

Figure 5. The effects of peptide therapy on serum T4 levels were evaluated. The measurements were performed in Ad-TSHR–immunized mice treated by either 4-weekly injections with vehicle (0.9% NaCl; "Graves no therapy" group; n = 25 mice) or 1 mg/kg body weight of peptide 836 (n = 12 mice), peptide 829 (n = 13 mice), TSHR-Fc (n = 18 mice), or control peptide 835 (n = 13 mice). In addition, age-matched immunologically naive unimmunized mice ("healthy"; n = 19 mice) were investigated. Data are presented as mean ± standard error of mean. Significance over time was tested by ANOVA of groups at given time points and controlled by ANOVA for repeated measurements within one group, followed by least significant difference *post hoc* testing. $*P < 0.05$ and $**P < 0.005$ compared with the TSHR-immunized group treated with only NaCl ("Graves no therapy" groups).

for peptide 835, whose sequence was derived from the seventh loop are also shown).

Pathohistological changes of the orbits

A histological investigation of retro-orbital fibrosis was performed on most animals. Coronary sections of orbital and retro-orbital tissues were evaluated after Masson's staining [Fig. 6(a)]. In nine Ad-TSHR–treated mice, a substantial increase of retro-orbital fibrosis was observed on digitized image analysis (23), which was completely reversed in the peptide 836-treated mice [Fig. 6(b)]. Tissues from four of the treatment groups were analyzed; the sections from the other peptide-treated groups were not processed, because these peptides did not result in improvement of the other investigated parameters.

ECG to determine heart rates

Starting from the third immunization, a substantial increase in heart rate in the hyperthyroid Ad-TSHR immunized group was observed [Fig. 7(a)]. In contrast, the heart rate in the native, healthy group was only mildly increased at an older age and had not changed significantly.

With consecutive Ad-TSHR immunizations, an additional strong increase in heart rate in the hyperthyroid vehicle-treated group was observed. In contrast, the peptide 836-treated and TSHR-Fc–treated animals showed no further increase and had substantially decreased heart rates at rest at later time points. The mean heart rates of these two treated groups were close to that of the healthy animal group. In contrast, the peptide 829-treated mice showed a trend that did not reach statistical significance. Also, the other tested cyclic peptides derived from the structure of the TSHR A domain did not show any effects (an example of an inactive control is shown in the results for peptide 835).

Heart weights

Macroscopic investigation and preparation of mouse hearts on necropsy revealed significantly increased heart weights in the Ad-TSHR–immunized groups [Fig. 7(b)]. In contrast, the peptide 836-treated mice showed significantly reduced heart weights. The peptide 829-treated and TSHR-Fc–treated animals showed a trend toward a reduced heart weight that did not reach statistical significance. Also, other tested cyclic peptides derived from the structure of the TSHR A domain did not show any effects (an example of an inactive control is shown by the results for peptide 835). Additionally, calculation of myocardial volumes by summing the digitized cross-sectional left ventricular areas from six consecutive

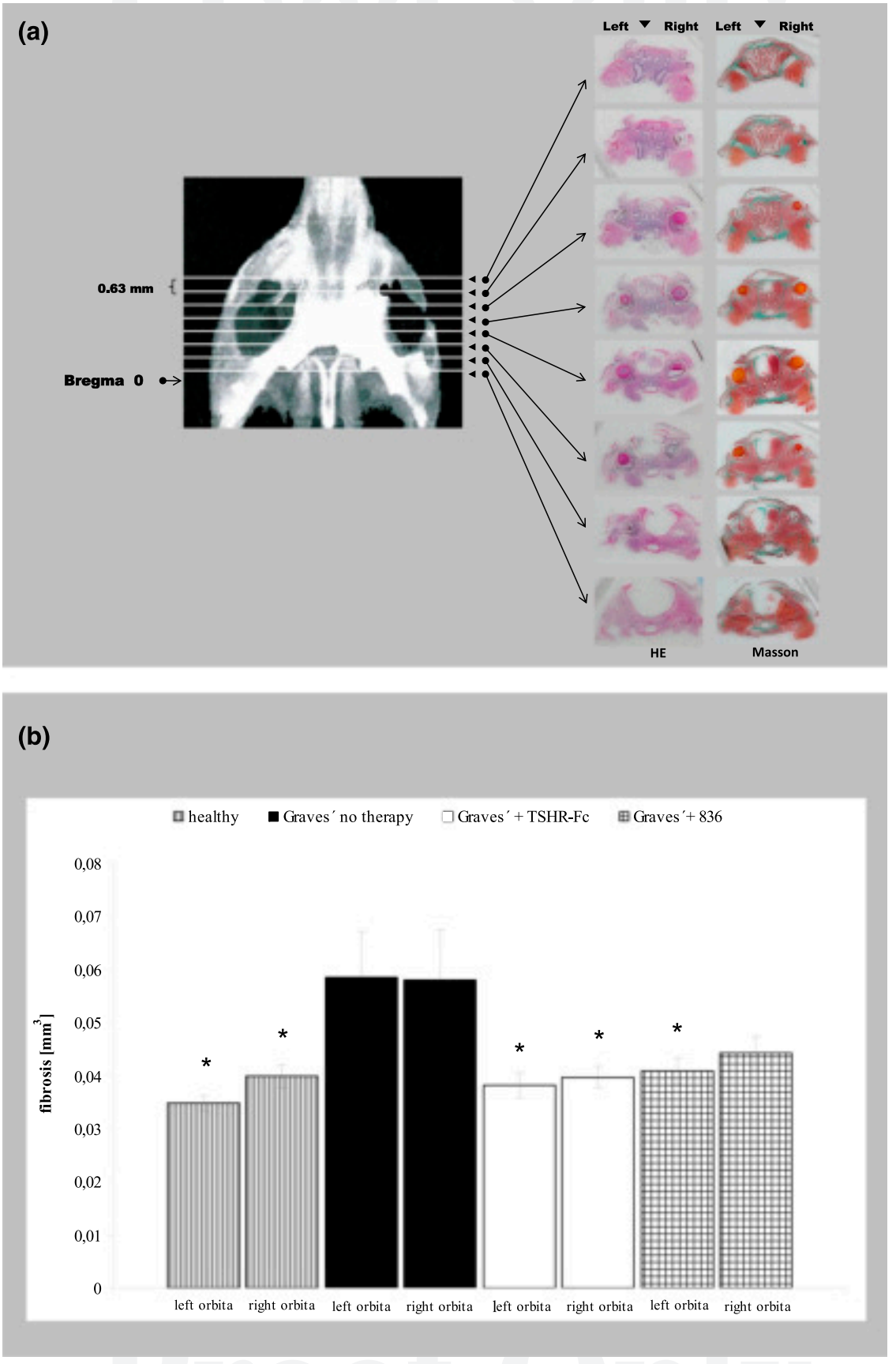

4C

Figure 6. Histological investigation of orbital sections. (a) Representative macroscopic images of coronary sections of a mouse orbit and neighboring tissues. The sections were taken at defined distances from the mouse bregma. Interstitial connective tissue was then stained in green (Masson's trichrome stain). For clarity, both hematoxylin and eosin (HE)-stained sections (left) and Masson's trichrome-stained sections (right) are

sections that were evenly distributed across the fixated hearts showed increased left ventricular volumes in the vehicle-treated mice. In contrast, the peptide 836-treated and TSHR-Fc–treated mice had significantly reduced ventricular myocardial volumes [Fig. 7(c)]. Because of the unavailability of some fine histologic sections, analysis of this parameter in mice treated with other peptides could not be completed.

Studies in immunologically naïve mice

All immunologically naive mice tolerated administration of either 1 mg/kg body weight of cyclic peptide 836 or vehicle (NaCl) every 4 weeks for 6 months equally well. No pathological clinical findings were observed. The generation of anti-TSHR antibodies was not observed in any of the six animals treated with cyclic peptide 836 during the 6-month period; all measured titers were less than background. Thus, no immune response to either peptide was documented. Because of the lack of efficacy in the disease model, administration of peptide 829 in naive mice was omitted.

In contrast, one naïve mouse, which had been treated with 1 mg/kg body weight TSHR-Fc developed clinical signs of allergy immediately after four administrations. In this mouse and two other mice treated with 1 mg/kg TSHR-Fc (total, 3 of 6 TSHR-Fc–treated naive mice), anti-TSHR antibody titers greater than the cutoff limit (as defined in the control groups) occurred after three administrations and were also observed with the continuing monthly measurements. At the end of the 6-month observation period, the average anti-TSHR antibody titers in all naive mice that had received TSHR-Fc were significantly ($P < 0.001$) greater than those in the cyclic peptide-treated or vehicle-treated control mice.

In vitro studies

To investigate whether the cyclic peptides or TSHR-Fc had a direct scavenging effect on anti-TSHR antibodies, we used a modified third-generation titer assay [Fig. 8(a)]. The fusion protein TSHR-Fc (100 μg/mL) significantly reduced anti-TSHR antibody titers (determined by measuring M22 binding, which was added at a final concentration of 10 ng/mL, to its substrate). No such effect was observed with the cyclic peptides. Also, we investigated the cAMP-stimulating potencies in TSHR-expressing test cells, which yielded qualitatively comparable results [Fig. 8(b)].

Discussion

In the present study, we found that the specific cyclic peptide 836, which mimics the eighth cylindrical loop of the LRD of TSHR markedly reduced thyroid hyperplasia and histological alterations in a long-term mouse model of Graves disease. Elevated T4 levels had reverted to normal values starting 15 weeks after the initiation of peptide therapy. We also found that retro-orbital fibrosis, tachycardia, and cardiac hypertrophy were consistently reduced after repeated administration of these peptides. Although treatment with both cyclic peptide 836 and a fully antigenic fusion protein of the TSHR A subunit and IgG-Fc (TSHR-Fc) suppressed or, at least stabilized, the titers of TSHR-binding antibodies despite continuing immunizations, TSHR-Fc treatment led to clinical signs of allergic reactions in immunized mice. The allergic reactions required treatment with the antihistaminic agent clemastine. Comparing the two treatments in naive mice reconfirmed that the shorter cyclic peptides are not immunogenic on their own and that administration of TSHR-Fc led to induction of anti-TSHR antibodies and clinical signs of allergy in some animals. In contrast, treatment with the cyclic peptide 829 designed in analogy to another loop of the subunit A of TSHR only resulted in small, nonsignificant trends, and other peptides mimicking the remaining loops of the TSHR LRD did not result in any effects at all.

The addition of serum samples from *in vivo* treated mice to measure the maximum TSHR-induced cAMP levels in test cells showed that this parameter was not affected by therapy with either peptide 836 or TSHR-Fc. Spiking of TSHR-Fc, but not of the cyclic peptides, to anti-TRSR antibodies *ex vivo* resulted in a reduction of titer and activity, suggesting antibody-scavenging capacity of TSHR-Fc but not of the peptides. Their interaction with immune mechanisms *in vivo* might be based on direct B-cell or T-cell effects.

In extension to previous work by others (reviewed by McLachlan *et al.* [27], Nagayama [28], and Kaneda *et al.* [29]) and our previous reports (22, 23), we have reconfirmed that long-term repeated Ad-induced TSHR A subunit immunization in mice leads to a long-term

Figure 6. (Continued). shown next to each other. (b) Effects of peptide therapy on severity of retro-orbital fibrosis were evaluated in histological sections of all available animals. The measurements were performed in Ad-TSHR–immunized mice treated by injections with vehicle (0.9% NaCl; "Graves no therapy" group; n = 9 mice) or 1 mg/kg body weight of peptide 836 (n = 11 mice) or TSHR-Fc (n = 11 mice). In addition, age-matched immunologically naive unimmunized mice ("healthy"; n = 10 mice) were investigated. The mean ± standard error of mean total fibrosis volumes of each right and left orbit, as assessed by digitized image analysis of all sections and consecutive integrations are shown. Differences between groups were tested by ANOVA. *$P < 0.05$ compared with TSHR-immunized group treated with only NaCl ("Graves no therapy" group).

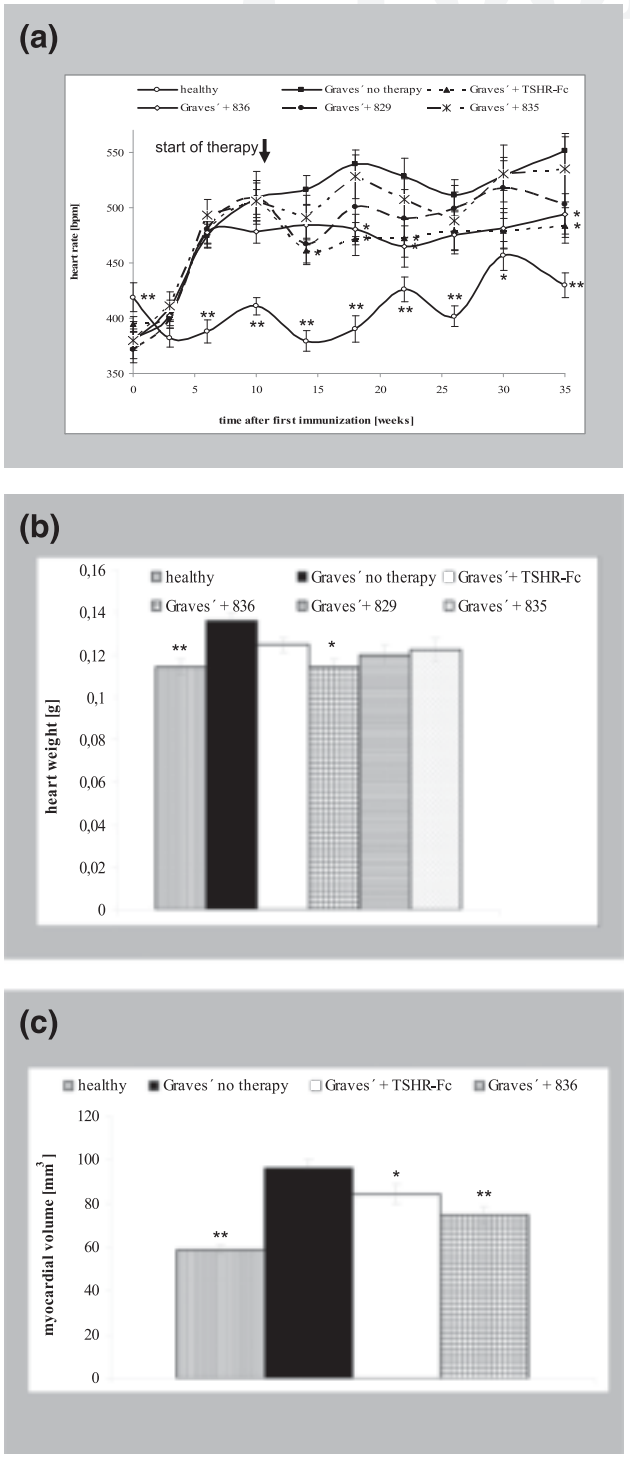

Figure 7. The effects of peptide therapy on (a) heart rates at various times during the experiment and on (b) heart weight and (c) cardiac ventricular volume at the end of the experiment were evaluated in all mice. The measurements were performed in Ad-TSHR–immunized mice treated by injections with vehicle (0.9% NaCl; "Graves no therapy" group; n = 25 mice) or 1 mg/kg body weight of peptide 836 (n = 12 mice), peptide 829 (n = 13 mice), or TSHR-Fc (n = 18 mice). In addition, age-matched immunologically naive unimmunized mice ("healthy"; n = 19 mice) were investigated. Data presented as mean ± standard error of mean. Significance over time was tested by ANOVA of groups at given time points and controlled by ANOVA for repeated measurements within one group, followed by least significant difference *post hoc* testing. $*P < 0.05$ and $**P < 0.005$ compared with TSHR-immunized group treated with only NaCl ("Graves no therapy" group).

model of Graves disease. In the present study, this model was used to test innovative therapeutic approaches. Previous studies of Ad-TSHR–immunized mice had established that the model can be used to investigate therapeutic interventions. An early specific immune therapeutic approach in mouse models of Graves disease relied on intranasal administration of linear peptides as T-cell epitopes; however, this did not prove successful (30). Alternatively, a soluble form of the TSHR A domain (expressed as his-tagged protein in CHO cells) was shown to induce tolerance in mice when given before subsequent Ad-TSHR immunization (31). However, a single intramuscular or subcutaneous injection of this protein was not effective against established disease in this short-term model of Ad-TSHR immunization. The anti-TSHR titers did not decrease but, rather, increased, and the T4 levels were unaltered in these mice. The differences between that protocol and the one used in our study are obvious. We used repeated intravenous injections of a dimeric TSHR-Fc fusion protein with a treatment duration and follow-up period of several months. This protocol allowed us to detect the long-term effects on the immune system. Also, we used repeated injections of TSHR-Fc with concomitant administration of the antihistaminic drug clemastine, because clinical signs of an allergic reaction had occurred in some TSHR-Fc–treated mice. This allergic reaction might have resulted from alien recognition of the fully human protein in mice; however, it could also have resulted from a genuine immune interaction of the anti-TSHR antibodies with this agent. In some naive mice, TSHR-Fc also induced an immune response, although none of the shorter cyclic peptides did. Therefore, therapy using TSHR-Fc currently seems less promising than that with the cyclic peptide 836, which did not cause any such symptoms.

In another study, intraperitoneal or intramuscular challenges of Ad-TSHR on neonatal mice induced tolerance against further immunizations in adulthood (32). However, such a virus-mediated prophylaxis could be difficult to establish in human medicine. In the same disease model, less specific immunotherapies also proved successful, including a mouse anti-CD20 antibody, an analog of rituximab (33) (see previous comments on clinical studies) and the B-cell activating factor fusion protein TACI-Fc (atacicept) (21), which can block B-cell activing factor (B-lymphocyte stimulator) on these cells. Q:15

Further work by Furmaniak *et al.* (34) identified inhibitory monoclonal TSHR-binding antibodies such as

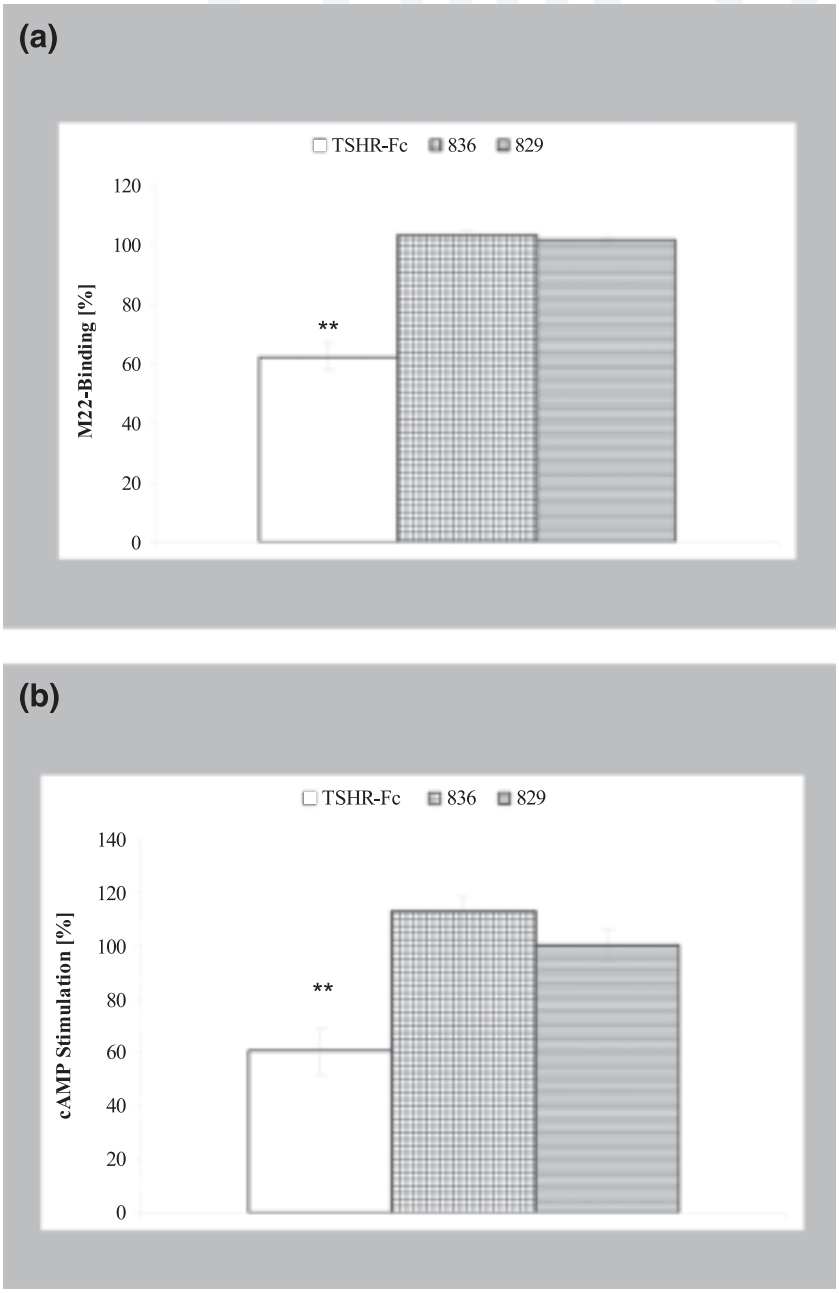

Figure 8. Effect of peptides on (a) anti-TSHR antibody titers and (b) cAMP stimulation in TSHR-expressing test cells *ex vivo* (anti-TSHR antibody-positive serum samples). Each measurement was performed in four samples. Results are shown as the percentage of untreated controls with standard error of the mean. Significance was tested by ANOVA between groups, followed by least significant difference *post hoc* testing. $^{**}P < 0.001$ compared with controls.

K1-70, which were isolated from patient blood and competed for the stimulatory action of autoantibodies of patients with Graves disease. They can counteract hyperthyroid states in M22-injected rats (34). In addition, small molecule TSHR antagonists were conceived but to date have only been tested *ex vivo* and in healthy mice (35–37). These compounds, such as ANTAG3, are active but seemingly only at fairly high *in vivo* doses. In addition, all have some cross-reactivity with the luteinizing or follicle-stimulating hormone receptors (34), and their toxicological characterizations have not yet been reported.

In contrast and/or complementary to these TSHR-blocking approaches by allosteric modulation, the use of cyclic peptides such as 836 does not incur direct receptor antagonism (see the section "*In vitro* results"), which should result in a favorable side effect profile. This issue requires clarification in future studies.

An alternative approach to treat severe cases of Graves disease (3, 6) is offered by specific immune therapies established for >100 years for a variety of allergic autoimmune conditions (reviewed by Larché and Wraith [10] and Soyka *et al.* [11]). Increasingly, recombinant peptides have been used for these hyposensitization therapies, which offer substantial advantages over the classic raw allergen extracts (10, 12, 13, 38). As a novel option, intravenous administration of relatively high doses of immunogen-mimicking cyclic peptides has been established for the treatment of anti–G protein–coupled receptor-mediated autoimmune disease (14–18). In the present study, we investigated a similar approach for anti-TSHR–mediated disease by providing cyclic peptides that mimic the tertiary structure of the cylindrical loops of the leucine-rich repeat domain of the TSHR. These peptides were systematically tested for their potency to treat clinical disease manifestations in Ad-TSHR–immunized diseased mice. We found that one such peptide, which had been designed in analogy of the eighth cylindrical loop of the leucine-rich repeat domain of the TSHR, was specifically and therapeutically active. Another showed weak, questionable activity, and all other tested peptides showed no signs of activity. This finding implies that Graves autoimmunity depends on specific parts of the receptor molecule, at least in this mouse model of disease.

Concerning the potential modes of action of such cyclic peptides, a variety of hypotheses can be considered. The immune-modulating potency of cyclic peptides that mimic parts of the antigen might depend on the property

that allows them to be presented to the immune system via major histocompatibility class II-dependent antigen-presenting cells without a costimulatory signal, thereby, reducing immune activation. In this process, the possible intermediate steps include the induction of T regulatory lymphoid cells, the suppression of T helper 1 cells and promotion of T helper 2 cell responses. These phenomena have been described during hyposensitization with specific peptides, such as the major cat allergen Fel D1 (13, 39). Parallel induction of blocking IgG4 vs IgE has been documented (13, 38) but cannot be studied in mice (11).

An alternative explanation for the observed phenomena would be complete and direct B-cell anergy by affecting peripheral lymphoid organs, which can also be observed with the broader, less specific approaches of generally blocking costimulatory signals or B-cell depletion (reviewed by Murphy *et al.* [40] and Blank and Shoenfeld [41]). This is also assumed to be the major effect of cyclic peptides, which suppress anti-β1AR antibodies raised in rats (16). Owing to the various histological assessments that were performed, we were not able to harvest spleen cells with sufficient quality for further immunological investigation from the mice studied in our protocol. We plan to measure these parameters in future studies of the same peptides.

Regarding the anti-TSHR antibody titer assays, the current reference standard third-generation immunoassay, which detects the ability of the respective mouse sera to inhibit the binding of the monoclonal Graves patient antibody M22 to the TSHR (RSR-Cobas Roche), is most often used to identify Graves disease in humans. This assay was reported to identify patients with Graves disease with a specificity and sensitivity of >97% (42, 43). Our study has documented the effects of peptide therapies on the anti-TSHR antibody titers, which were measured using the same assay used in human patients. In contrast, the peptides showed no or very little effects on TSHR-mediated cAMP stimulatory potency during progressive therapy (Fig. 3); other secondary messenger pathways coupled to TSHR might be involved, such as Gq-phospholipase C or even inhibitory regulative G protein. We experienced similar findings when we sought to establish the best suited assay to measure relevant anti-β1AR antibodies (44).

This finding is not as paradoxical as it might seem, because specific immune therapies for allergies often do not show overall changes in antigen-specific antibody titers, although they are clinically effective. Also, it might have resulted from a shift of specific antibody subtypes or alteration of antigen-presenting properties of B-cell subpopulations. We will investigate this interesting aspect in further studies.

In addition, we investigated orbital histologic findings and quantified retro-orbital fibrosis using digitized image analysis, which represents an important hallmark of clinical disease in humans. It has been shown to be altered in previous studies using electroporation and plasmid gene transfer (45, 46) but not during short-term Ad-TSHR immunization (47). In contrast, our previous pilot study showed that Graves orbitopathy develops if Ad immunizations are maintained for several months (23). The administration of our cyclic peptides induced a substantial reduction of retro-orbital fibrosis in the present study. This finding represents an interesting confirmation of findings from previous preclinical studies using Graves disease models, because, to the best of our knowledge, such a therapeutic effect has not yet been shown in animal models. However, Graves ophthalmopathy in humans is especially difficult to treat.

We also investigated the effect of these peptides on the cardiac manifestations and complications of Graves disease. Tachycardia is a reliable marker of disease severity in hyperthyroid patients (48, 49). ECG monitoring for 24 hours showed that the heart rate is constantly increased during the day (49). Therefore, we sought to examine whether the investigated immune treatments can also affect the clinically important cardiac involvement in this animal model. Regular ECG readings were used to detect the effect on the heart rate. Treatment with either TSHR-Fc or peptide 836 significantly decreased the tachycardia that had progressively developed in untreated TSHR-immunized mice over 3 to 9 months.

In conclusion, the results of the present study have shown that treatment of clinical disease manifestations in this mouse model of Graves disease led to marked improvement of all disease parameters. TSHR-Fc resulted in direct antibody scavenging *ex vivo* but induced allergic reactions in some animals *in vivo*. The leucine-rich repeat loop-mimicking cyclic peptide 836 was equally effective *in vivo* but did not show this *ex vivo* effect. Because it mimics a part of the antigenic receptor, it might be presented to the immune system via major histocompatibility class II-dependent antigen-presenting cells, thereby reducing immune activation. Alternatively, direct induction of immune mechanisms *in vivo*, such as B-cell anergy in peripheral lymphoid tissues, might account for this effect (41).

Acknowledgments

Address all correspondence and requests for reprints to: Martin Ungerer, MD, Procorde-advanceCOR, Fraunhofer Strasse 9a, D 82152 Martinsried, Germany. E-mail: ungerer@procorde.com.

Disclosure Summary: The authors have nothing to disclose.

References

1. Weetman AP. Graves' disease. *N Engl J Med*. 2000;**343**(17):1236–1248.
2. Ross DS. Radioiodine therapy for hyperthyroidism. *N Engl J Med*. 2011;**364**(6):542–550.
3. Sundaresh V, Brito JP, Wang Z, Prokop LJ, Stan MN, Murad MH, Bahn RS. Comparative effectiveness of therapies for Graves' hyperthyroidism: a systematic review and network meta-analysis. *J Clin Endocrinol Metab*. 2013;**98**(9):3671–3677.
4. Abraham-Nordling M, Törring O, Hamberger B, Lundell G, Tallstedt L, Calissendorff J, Wallin G. Graves' disease: a long-term quality-of-life follow up of patients randomized to treatment with antithyroid drugs, radioiodine, or surgery. *Thyroid*. 2005;**15**(11):1279–1286.
5. Bahn RS. Graves' ophthalmopathy. *N Engl J Med*. 2010;**362**(8):726–738.
6. Stan MN, Garrity JA, Carranza Leon BG, Prabin T, Bradley EA, Bahn RS. Randomized controlled trial of rituximab in patients with Graves' orbitopathy. *J Clin Endocrinol Metab*. 2015;**100**(2):432–441.
7. El Fassi D, Nielsen CH, Bonnema SJ, Hasselbalch HC, Hegedüs L. B lymphocyte depletion with the monoclonal antibody rituximab in Graves' disease: a controlled pilot study. *J Clin Endocrinol Metab*. 2007;**92**(5):1769–1772.
8. Heemstra KA, Toes RE, Sepers J, Pereira AM, Corssmit EP, Huizinga TWJ, Romijn JA, Smit JW. Rituximab in relapsing Graves' disease, a phase II study. *Eur J Endocrinol*. 2008;**159**(5):609–615.
9. Salvi M, Vannucchi G, Currò N, Campi I, Covelli D, Dazzi D, Simonetta S, Guastella C, Pignataro L, Avignone S, Beck-Peccoz P. Efficacy of B-cell targeted therapy with rituximab in patients with active moderate to severe Graves' orbitopathy: a randomized controlled study. *J Clin Endocrinol Metab*. 2015;**100**(2):422–431.
10. Larché M, Wraith DC. Peptide-based therapeutic vaccines for allergic and autoimmune diseases. *Nat Med*. 2005;**11**(4 Suppl) S69–S76.
11. Soyka MB, van de Veen W, Holzmann D, Akdis M, Akdis CA. Scientific foundations of allergen-specific immunotherapy for allergic disease. *Chest*. 2014;**146**(5):1347–1357.
12. Valenta R, Ferreira F, Focke-Tejkl M, Linhart B, Niederberger V, Swoboda I, Vrtala S. From allergen genes to allergy vaccines. *Annu Rev Immunol*. 2010;**28**:211–241.
13. Marth K, Focke-Tejkl M, Lupinek C, Valenta R, Niederberger V. Allergen peptides, recombinant allergens and hypoallergens for allergen-specific immunotherapy. *Curr Treat Options Allergy*. 2014;**1**:91–106.
14. Jahns R, Boivin V, Hein L, Triebel S, Angermann CE, Ertl G, Lohse MJ. Direct evidence for a β_1-adrenergic receptor-directed autoimmune attack as a cause of idiopathic dilated cardiomyopathy. *J Clin Invest*. 2004;**113**(10):1419–1429.
15. Freedman NJ, Lefkowitz RJ. Anti-$\beta_{(1)}$-adrenergic receptor antibodies and heart failure: causation, not just correlation. *J Clin Invest*. 2004;**113**(10):1379–1382.
16. Boivin V, Beyersdorf N, Palm D, Nikolaev VO, Schlipp A, Müller J, Schmidt D, Kocoski V, Kerkau T, Hünig T, Ertl G, Lohse MJ, Jahns R. Novel receptor-derived cyclopeptides to treat heart failure caused by anti-β1-adrenoceptor antibodies in a human-analogous rat model. *PLoS One*. 2015;**10**(2):e0117589.
17. Münch G, Boivin-Jahns V, Holthoff HP, Adler K, Lappo M, Truöl S, Degen H, Steiger N, Lohse MJ, Jahns R, Ungerer M. Administration of the cyclic peptide COR-1 (phase I study): ex vivo measurements of anti-β1-adrenergic receptor antibody neutralization and of immune parameters. *Eur J Heart Fail*. 2012;**14**(11):1230–1239.
18. Störk S, Plotnikov AN, Peters G, Davies BE, Nnane I, Rivas D, Tesfaye F, Kääb S, Bauer A, Luchner A, Ungerer M, Jahns R, Lohse MJ, Ertl G. Effects of JNJ-54452840, an anti-β1 receptor antibody cyclopeptide in heart failure patients: a randomized, double-blind, parallel-group, phase-2 pilot study. *Cardiovac Pharmacol Open*. 2016;**5**:190.
19. Nagayama Y, Kita-Furuyama M, Ando T, Nakao K, Mizuguchi H, Hayakawa T, Eguchi K, Niwa M. A novel murine model of Graves' hyperthyroidism with intramuscular injection of adenovirus expressing the thyrotropin receptor. *J Immunol*. 2002;**168**(6):2789–2794.
20. Chen CR, Pichurin P, Nagayama Y, Latrofa F, Rapoport B, McLachlan SM. The thyrotropin receptor autoantigen in Graves disease is the culprit as well as the victim. *J Clin Invest*. 2003;**111**(12):1897–1904.
21. Gilbert JA, Kalled SL, Moorhead J, Hess DM, Rennert P, Li Z, Khan MZ, Banga JP. Treatment of autoimmune hyperthyroidism in a murine model of Graves' disease with TNF family ligand inhibitors suggests a key role for B cell activating factor in disease pathology. *Endocrinology*. 2006;**147**(10):4561–4568.
22. Holthoff HP, Goebel S, Li Z, Faßbender J, Reimann A, Zeibig S, Lohse MJ, Münch G, Ungerer M. Prolonged TSH receptor A subunit immunization of female mice leads to a long-term model of Graves' disease, tachycardia, and cardiac hypertrophy. *Endocrinology*. 2015;**156**(4):1577–1589.
23. Ungerer M, Fassbender J, Li Z, Münch G, Holthoff HP. Review of mouse models of Graves' disease and orbitopathy—novel treatment by induction of tolerance. *Clin Rev Allerg Immunol*. 2017;**52**:182.
24. Parmentier M, Libert F, Maenhaut C, Lefort A, Gérard C, Perret J, Van Sande J, Dumont JE, Vassart G. Molecular cloning of the thyrotropin receptor. *Science*. 1989;**246**(4937):1620–1622.
25. Nagayama Y, Kaufman KD, Seto P, Rapoport B. Molecular cloning, sequence and functional expression of the cDNA for the human thyrotropin receptor. *Biochem Biophys Res Commun*. 1989;**165**(3):1184–1190.
26. Dahab GM, Kheriza MM, El-Beltagi HM, Fouda AM, El-Din OA. Digital quantification of fibrosis in liver biopsy sections: description of a new method by Photoshop software. *J Gastroenterol Hepatol*. 2004;**19**(1):78–85.
27. McLachlan SM, Nagayama Y, Rapoport B. Insight into Graves' hyperthyroidism from animal models. *Endocr Rev*. 2005;**26**(6):800–832.
28. Nagayama Y. Graves' animal models of Graves' hyperthyroidism. *Thyroid*. 2007;**17**(10):981–988.
29. Kaneda T, Honda A, Hakozaki A, Fuse T, Muto A, Yoshida T. An improved Graves' disease model established by using in vivo electroporation exhibited long-term immunity to hyperthyroidism in BALB/c mice. *Endocrinology*. 2007;**148**(5):2335–2344.
30. Arima T, Shimojo N, Yamaguchi K, Tomiita M, Kohn LD, Kohno Y. Enhancement of experimental Graves' disease by intranasal administration of a T cell epitope of the thyrotropin receptor. *Clin Immunol*. 2008;**127**(1):7–13.
31. Misharin AV, Nagayama Y, Aliesky HA, Mizutori Y, Rapoport B, McLachlan SM. Attenuation of induced hyperthyroidism in mice by pretreatment with thyrotropin receptor protein: deviation of thyroid-stimulating to nonfunctional antibodies. *Endocrinology*. 2009;**150**(8):3944–3952.
32. Wu L, Xun L, Yang J, Xu L, Tian Z, Gao S, Zhang Y, Hou P, Shi B. Induction of murine neonatal tolerance against Graves' disease using recombinant adenovirus expressing the TSH receptor A-subunit. *Endocrinology*. 2011;**152**(3):1165–1171.
33. Ueki I, Abiru N, Kobayashi M, Nakahara M, Ichikawa T, Eguchi K, Nagayama Y. B cell-targeted therapy with anti-CD20 monoclonal antibody in a mouse model of Graves' hyperthyroidism. *Clin Exp Immunol*. 2011;**163**(3):309–317.
34. Furmaniak J, Sanders J, Núñez Miguel R, Rees Smith B. Mechanisms of action of TSHR autoantibodies. *Horm Metab Res*. 2015;**47**(10):735–752.
35. Neumann S, Eliseeva E, McCoy JG, Napolitano G, Giuliani C, Monaco F, Huang W, Gershengorn MC. A new small-molecule

antagonist inhibits Graves' disease antibody activation of the TSH receptor. *J Clin Endocrinol Metab*. 2011;**96**(2):548–554.
36. van Zeijl CJJJ, van Koppen CJ, Surovtseva OV, de Gooyer ME, Plate R, Conti P, Karstens WJ, Timmers M, Saeed P, Wiersinga WM, Miltenburg AMM, Fliers E, Boelen A. Complete inhibition of rhTSH-, Graves' disease IgG-, and M22-induced cAMP production in differentiated orbital fibroblasts by a low-molecular-weight TSHR antagonist. *J Clin Endocrinol Metab*. 2012;**97**(5): E781–E785.
37. Neumann S, Place RF, Krieger CC, Gershengorn MC. Future prospects for the treatment of Graves' hyperthyroidism and eye disease. *Horm Metab Res*. 2015;**47**(10):789–796.
38. Creticos PS. Advances in synthetic peptide immuno-regulatory epitopes. *World Allergy Organ J*. 2014;**7**(1):30.
39. Jutel M, Akdis CA. Immunological mechanisms of allergen-specific immunotherapy. *Allergy*. 2011;**66**(6):725–732.
40. Murphy K, Travers P, Walport M. *Janeways's Immunobiology*. New York: Garland Science Editors; 2008:347–348.
41. Blank M, Shoenfeld Y. B cell targeted therapy in autoimmunity. *J Autoimmun*. 2007;**28**(2-3):62–68.
42. Kamijo K, Ishikawa K, Tanaka M. Clinical evaluation of 3rd generation assay for thyrotropin receptor antibodies: the M22-biotin-based ELISA initiated by Smith. *Endocr J*. 2005;**52**(5): 525–529.
43. Tozzoli R, Bagnasco M, Giavarina D, Bizzaro N. TSH receptor autoantibody immunoassay in patients with Graves' disease: improvement of diagnostic accuracy over different generations of methods: systematic review and meta-analysis. *Autoimmun Rev*. 2012;**12**(2):107–113.
44. Holthoff HP, Zeibig S, Jahns-Boivin V, Bauer J, Lohse MJ, Kääb S, Clauss S, Jahns R, Schlipp A, Münch G, Ungerer M. Detection of anti-β1-AR autoantibodies in heart failure by a cell-based competition ELISA. *Circ Res*. 2012;**111**(6):675–684.
45. Zhao SX, Tsui S, Cheung A, Douglas RS, Smith TJ, Banga JP. Orbital fibrosis in a mouse model of Graves' disease induced by genetic immunization of thyrotropin receptor cDNA. *J Endocrinol*. 2011;**210**(3):369–377.
46. Moshkelgosha S, So PW, Deasy N, Diaz-Cano S, Banga JP. Cutting edge: retrobulbar inflammation, adipogenesis, and acute orbital congestion in a preclinical female mouse model of Graves' orbitopathy induced by thyrotropin receptor plasmid in vivo electroporation. *Endocrinology*. 2013;**154**:3008–3015.
47. Banga JP, Moshkelgosha S, Berchner-Pfannschmidt U, Eckstein A. Modeling Graves' orbitopathy in experimental Graves' disease. *Horm Metab Res*. 2015;**47**(10):797–803.
48. Klein I, Ojamaa K. Thyroid hormone and the cardiovascular system. *N Engl J Med*. 2001;**344**(7):501–509.
49. von Olshausen K, Bischoff S, Kahaly G, Mohr-Kahaly S, Erbel R, Beyer J, Meyer J. Cardiac arrhythmias and heart rate in hyperthyroidism. *Am J Cardiol*. 1989;**63**(13):930–933.

AUTHOR QUERIES

AUTHOR PLEASE ANSWER ALL QUERIES 1

NOTE: The figures that you submitted in color have been processed to appear as color online and color in print. If you wish to have any of these figures instead appear as color online and black and white in print, please indicate the figures for which you wish this change to apply. If you choose to convert a figure that you originally submitted in color to appear as black and white in print, you must revise color descriptors to ensure that any text references and captions to that figure remain informative for readers of the print version.

Q: 1_Please confirm that given names and surnames are identified properly by the colors indicated. Colors will not appear in print or online, and are for proofing and coding purposes only to ensure proper indexing on PubMed.

Q: 2_Please verify all author names and affiliations.

Q: 3_The publisher conforms to the usage practice of the nonpossessive form of eponymous terms; all such terms have been edited accordingly throughout. Please confirm.

Q: 4_In the sentence beginning “In contrast, monthly injections,” please spell out Fc here at first and only use in text, if appropriate.

Q: 5_References 6 to 9 have been renumbered so their citations appear in numerical order; please check the renumbering for accuracy. Ref. 9 is now ref. 6.

Q: 6_Please clarify the phrase "The latter readout indicates" (perhaps "Examination of retro-orbital fibrosis will indicate the severity"?).

Q: 7_Any alternations between capitalization and/or italics in genetic terminology have been retained per the original manuscript. Please confirm that all genetic terms have been formatted properly throughout. (Note that the standard convention is to represent genes in italic font and proteins in roman font.)

Q: 8_Please confirm expansion of LRR as “leucine-rich repeat domain" in the phrase "loop of the TSHR leucine-rich repeat domain" or provide the correct expansion.

Q: 9_In the phrase " dimethylformamide (DMF; 5+12 minutes)," please clarify use of the plus sign (“5 to 12 minutes” or “5 × 12 minutes” meant?).

Q: 10_Please confirm addition of "v/v/v" to "95:5:3" in the phrase " deblocked by trifluoroacetic acid/water/thioanisole (95:5:3 v/v/v)" or edit as necessary.

Q: 11_Please confirm "every 3 weeks" and "every 4 weeks" (or edit as necessary, avoiding phrases such as "3-weekly") in the phrase "The study protocol used three….”

Q: 12_The citation of Figure 6A with the phrase "sections were collected at positions (compared with bregma 0) +0.63, +1.26, +1.89, +2.52, +3.15, +3.78, +4.41, and +5.04 mm" was

AUTHOR QUERIES

changed to "shown in later figure" per Journal style because the citation was clearly "early" and the correct citation for Figure 6a appears later in the article.

Q: 13_The citation to Figure 6A appears to be out of order.

Q: 14_Reference 26 was not cited in your original; it has been cited with ref. 25 (phrase "trichrome stains had been validated previously") as a placeholder. Please confirm citation or cite correctly in numerical order.

Q: 15_Please clarify which section is meant in the phrase "see previous comments on clinical studies."

Q: 16_In the sentence beginning "In this process," should we use "type 1 T helper" and "type 2 T helper" cells, rather than "T helper 1" and "T helper 2" cells?

Q: 17_Reference 49 was cited before references 41 onward so these references have been renumbered in the text and reference list. Also, ref. 41 was cited after refs. 42 and 43; ref. 49 is now ref. 41 and ref. 41 is now ref. 44.

Q: 18_Please confirm expansion of "Gi" as "inhibitory regulative G protein" in the phrase "such as Gq-phospholipase C or even inhibitory regulative G protein," or edit as necessary.

Q: 19_Please confirm expansion of LRR as "leucine-rich repeat" in the phrase "leucine-rich repeat loop-mimicking cyclic peptide 836" or edit as necessary.

Q: 20_Please verify the corresponding author's information.

Q: 21_Please confirm that no financial support was received.

Q: 22_Please confirm or edit as necessary definition of TMD as transmembrane domain in caption for Fig. 1.

Q: 23_Please confirm third column table head as added or edit as necessary.